The physiological structure of human C-reactive protein and its complex with phosphocholine

Darren Thompson[1], Mark B Pepys[2] and Steve P Wood[1]*

Background: Human C-reactive protein (CRP) is the classical acute phase reactant, the circulating concentration of which rises rapidly and extensively in a cytokine-mediated response to tissue injury, infection and inflammation. Serum CRP values are routinely measured, empirically, to detect and monitor many human diseases. However, CRP is likely to have important host defence, scavenging and metabolic functions through its capacity for calcium-dependent binding to exogenous and autologous molecules containing phosphocholine (PC) and then activating the classical complement pathway. CRP may also have pathogenic effects and the recent discovery of a prognostic association between increased CRP production and coronary atherothrombotic events is of particular interest.

Results: The X-ray structures of fully calcified C-reactive protein, in the presence and absence of bound PC, reveal that although the subunit β-sheet jellyroll fold is very similar to that of the homologous pentameric protein serum amyloid P component, each subunit is tipped towards the fivefold axis. PC is bound in a shallow surface pocket on each subunit, interacting with the two protein-bound calcium ions via the phosphate group and with Glu81 via the choline moiety. There is also an unexpected hydrophobic pocket adjacent to the ligand.

Conclusions: The structure shows how large ligands containing PC may be bound by CRP via a phosphate oxygen that projects away from the surface of the protein. Multipoint attachment of one planar face of the CRP molecule to a PC-bearing surface would leave available, on the opposite exposed face, the recognition sites for C1q, which have been identified by mutagenesis. This would enable CRP to target physiologically and/or pathologically significant complement activation. The hydrophobic pocket adjacent to bound PC invites the design of inhibitors of CRP binding that may have therapeutic relevance to the possible role of CRP in atherothrombotic events.

Addresses: [1]School of Biological Sciences, University of Southampton, Southampton SO16 7PX, UK and [2]Immunological Medicine Unit, Imperial College School of Medicine, Hammersmith Hospital, Du Cane Road, London W12 0NN, UK.

*Corresponding author.
E-mail: steve@soton.ac.uk

Key words: acute phase response, apoptosis, C1q, C-reactive protein, serum amyloid P component, phosphocholine

Received: **15 September 1998**
Revisions requested: **16 October 1998**
Revisions received: **16 November 1998**
Accepted: **15 December 1998**

Published: **29 January 1999**

Structure February 1999, **7**:169–177
http://biomednet.com/elecref/0969212600700169

Introduction

C-reactive protein (CRP) is a normal plasma protein, the circulating concentration of which rises dramatically in a cytokine-mediated response to most forms of tissue injury, infection and inflammation, and serum CRP values are widely measured in clinical practice as an objective index of disease activity [1,2]. CRP is a member of the evolutionarily ancient and stably conserved pentraxin family that includes serum amyloid P component (SAP) [3], an important constituent of the amyloid deposits that underlie a range of human diseases including Alzheimer's [4,5]. The conservation of the structure of CRP and of its calcium-dependent specific binding of ligands containing phosphocholine (PC) [6] and related substances, together with the failure thus far to detect any polymorphism or deficiency of CRP in man, argue strongly that CRP has an important physiological role. PC is universal in phospholipids in cell membranes and plasma lipoproteins, and is common in complex polysaccharides of plants, fungi and bacteria, whilst CRP also binds specifically to small nuclear ribonucleoprotein particles [7,8]. Ligand recognition and binding by CRP may thus contribute to a range of metabolic, scavenging and host-defence functions. The recent discovery of a significant prognostic association between increased levels of serum CRP and coronary heart disease, especially myocardial infarction, has greatly heightened interest in this classical acute phase reactant, but, importantly, the association with coronary disease is evident even at CRP levels previously considered normal [9–15].

The capacity of human CRP to activate complement [16–20] and to stimulate tissue-factor production [21–23] suggests that CRP may have pro-inflammatory and procoagulant effects, and we have proposed [9,13] that these may contribute to pathogenesis of the progression and thrombo-occlusive complications of atheroma. CRP may thus be a significant therapeutic target and its molecular structure–function relationships are therefore potentially of practical as well as theoretical importance.

Although CRP was originally crystallised in 1947 [24], forms suitable for high-resolution X-ray analysis have not previously been obtained [25]. The 3 Å resolution structure of partially calcium-loaded (one protomer in each pentamer contained no bound calcium) CRP (Brookhaven Protein Data Bank [PDB] code 1gnh) was published during the course of the present work [26], but it was based on incomplete data with poor processing statistics collected from 33 microcrystals grown from CRP destabilised by the removal of calcium.

Results and discussion

Structure determination

The crystal structure of CRP was determined by molecular replacement, using human serum amyloid P component as the search model [27], but with the two calcium ions per subunit deleted. The asymmetric unit of the CRP crystal, grown in the presence of excess calcium, contained two pentamers that allowed tenfold averaging to produce a good quality electron-density map that enabled model building. The final R factor of this structure was 18.6% (R free 23%) to a resolution of 3 Å.

The structure of CRP co-crystallised with PC and calcium was determined from a crystal form containing only one pentamer in the asymmetric unit. Again, molecular replacement was used, but this time the CRP structure determined from the previous crystal form was used as the search model. Although the cell dimensions from each of these crystal forms are very similar, they are in fact of different space groups with very different solvent volumes (ligand free 53%, PC-bound 76%) and this is why the molecular replacement was needed to solve the PC-bound structure. Initial electron-density maps produced showed density for one molecule of PC in each subunit, bound at the double calcium binding site. The final R factor of this structure was 19.6% (R free 24.2%) to a resolution of 2.5 Å. On final comparison of the two structures, we found that the packing of the unliganded structure with two molecules in the asymmetric unit was such that it would be very difficult to accommodate PC molecules bound to each subunit. Otherwise, the two structures are extremely similar (a root mean square [rms] difference of 0.29 Å), with only minor changes in the positions of sidechains involved in ligand binding and crystal contacts. For this reason, the following analysis of the structure of CRP applies to both structures.

The structure of the CRP protomer

As we predicted [28] from homology modelling based on the crystal structure of SAP, the CRP protomer is very similar to that of SAP; the Cα rms fit is 1.3 Å, but it drops to 0.83 Å when three divergent loops involving 19 residues are omitted from the calculation (Figure 1). The subunits consist of a two-layered β sheet with a flattened jellyroll topology. Two calcium ions are bound 4 Å apart by protein sidechains coming from loops collected at the concave face,

Figure 1

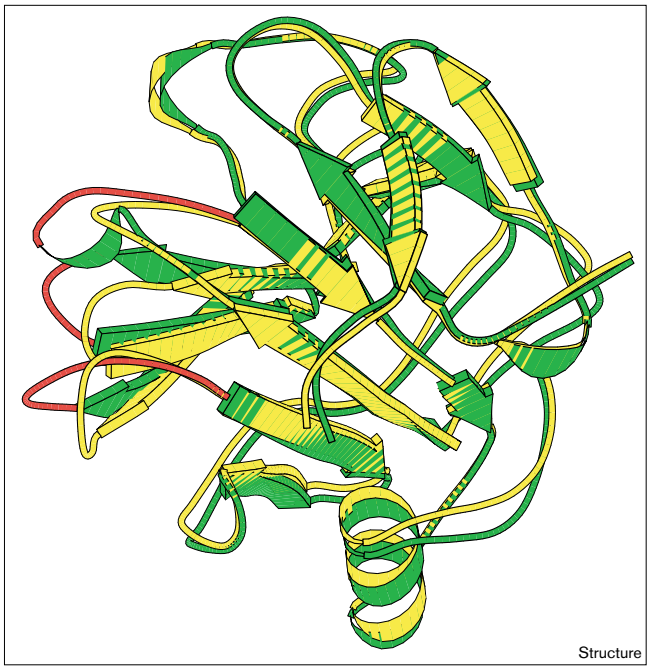

Ribbon overlay of an SAP protomer (yellow) and a CRP protomer (green) after a 22° rotation has been applied to the SAP protomer so as to bring the protomers into the same orientation. The red coloured CRP loops comprise residues 43–48, 68–72 and 85–91, which are the regions differing most between the two protomer structures.

designated B [29], of this sheet, and this is the site of ligand binding. The other face, designated A, carries a single α helix, and the pentameric disc shows five helices on one face and ten calcium ions on the other. The main structural differences in CRP occur in the longer β arches and loops linking top and bottom strands adjacent to the central pore of the pentamer (residues 43–48, 68–72, 85–91). Short helical regions form around residues 43 and 185.

On the A face of each subunit, there is a marked furrow (Figure 2a) that is accentuated in CRP by substitution of some smaller sidechains and by reorientation of others, and it defines a region 24 Å long, 7.5 Å deep and 12.4 Å wide. The side walls are constructed from Ser5, Arg6, Gln203, Pro206, Trp187, Arg188, Asn160, Gly177, Leu176, Tyr175, His95 and Asp112. The bottom is lined by Asn158, His38, Leu37, Val94 and Asp112. The appearance of this furrow in CRP is enhanced considerably by differences in the pentamer organisation compared to SAP. The furrows follow the curvature of the subunits and come closer together as they enter the pore at the centre of the pentamer. The outer part of the furrow is positively charged but the inner part terminates halfway through the pentamer pore at residue Asp112, providing a ring of negative charges lining the pore (Figure 2b). Mutagenesis experiments have

Figure 2

GRASP representation of **(a)** CRP pentamer illustrating the positions of the clefts present on the A surface; **(b)** CRP protomer illustrating the charge distribution in the cleft. Blue, positive charge; red, negative.

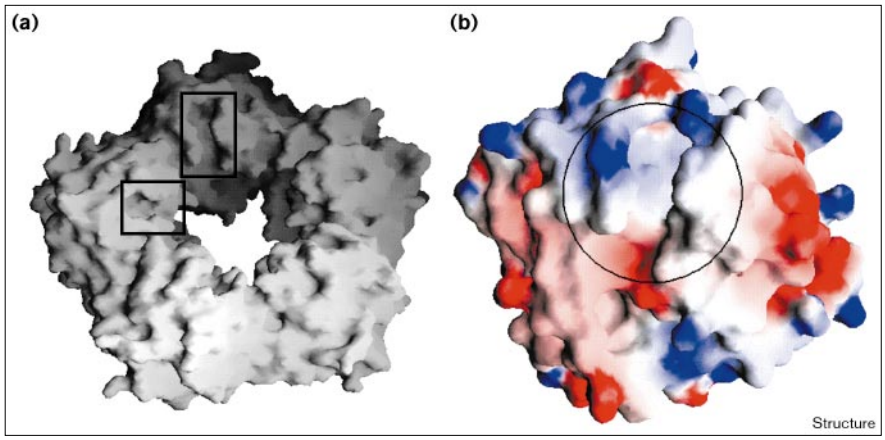

highlighted Asp112 as an important residue for recognition of C1q by CRP [30].

The structure of the CRP pentamer

In SAP, the core β sheets of each protomer are in a plane approximately normal to the fivefold axis. In contrast, each subunit in CRP for both crystal forms is rotated by *22°* towards the fivefold axis (Figure 3) such that the helices of face A are 5 Å closer to the axis and the calcium sites on face B move away by an equivalent amount. The rotational shift of *22°* observed between the orientations of SAP and CRP protomers was calculated by first superimposing the pentamers from both molecules such that the fivefold axes of the two proteins were parallel and equivalent protomers were superimposed. The equivalent protomers of CRP and SAP were then compared using LSQKAB (CCP4 suite) [31] to determine the rotational relationship between the two in polar angles. The rotation axis is roughly parallel to the long helix on the surface of the protomer and runs through the centre of mass of the subunit.

The interactions between subunits in the SAP pentamer involve van der Waals contacts and hydrogen bonding, and lead to 1650 $Å^2$ (20%) of buried surface per protomer. The contacts involve the open-core end of the β-sheet sandwich of one subunit with the N- and C-terminal strands of the next. A rather similar surface area is buried in CRP, but changes in sequence relative to SAP and the subunit rotation lead to small changes in the bonding pattern that must stabilise the rotated state of the subunits. For instance, residues Glu197 and Lys123 in CRP form an intermolecular ion pair not formed by Tyr195 and Gln121 in SAP. The CRP Asp155–Arg118 and Glu101–Lys201 ion pairs, however, correspond to Glu153–Lys116 and Glu99–Lys199 in SAP. When we impose the observed subunit rotation of CRP onto the SAP coordinates, there are surprisingly few major clashes, the most notable being between Val202 and Pro166 of the adjacent subunit. In CRP, the equivalent Leu204 moves to a new position and the mainchain path increasingly deviates from the equivalent region in rotated SAP beyond Pro202, away from the subunit interface. This leads to a marked reorganisation of the position of the Trp205 ring in CRP, compared to SAP Trp203 (Figure 4), resulting from a mainchain shift and a rotation of about 90° around the Cβ–Cγ bond, so that the ring stacks at a distance of 3.7 Å with the sidechain of His38 (corresponding to SAP Arg38) of the same subunit. In view of the modest surface area buried and the relative ease of interconverting the subunit packing arrangements it is possible that such movements represent a dynamic capacity of both molecules. Crystal packing forces may play a role in stabilising a particular arrangement and in all our crystal forms there are substantial face to face contacts between adjacent pentamers. Interestingly, such movements of the protomers redistribute the ligand-binding sites on the B face of the pentamer and might be of significance in multivalent binding to structures such as cell membranes, protein aggregates, or nucleic acid–protein complexes.

The calcium-binding site

The calcium-binding sites in the present CRP structures are organised in a similar fashion to those in SAP, but a number of differences in the protein ligands to the calcium ions help to explain known differences in the calcium affinity between the proteins. In SAP, there is distinct asymmetry in the ligand distribution such that site 1 calcium receives six protein ligands whereas site 2 calcium receives only three. In both sites, carboxylate or phosphate ligands provide one additional bond per metal atom. The larger site 2 pocket can accommodate a barium or cerium ion. Calcium ions wash out rather easily and the site is only partially occupied in the SAP crystal structure; it may exist in a partially calcium loaded form at physiological calcium concentrations in the absence of external ligands. The equivalent site 1 residues in CRP include Asp60, Asn61, Glu138, Asp140 and the mainchain carbonyl oxygen

Figure 3

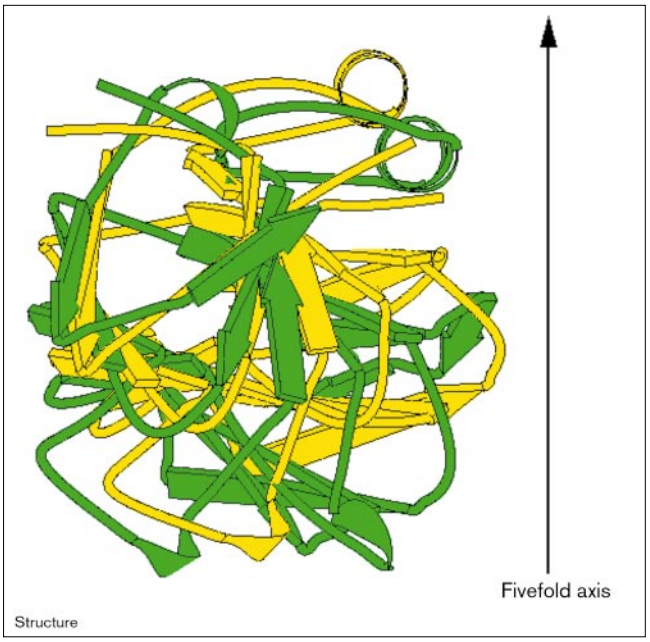

Ribbon overlay of an SAP protomer (yellow) and a CRP protomer (green) indicating the orientation of the protomers with respect to the fivefold axis of the pentamers.

Figure 4

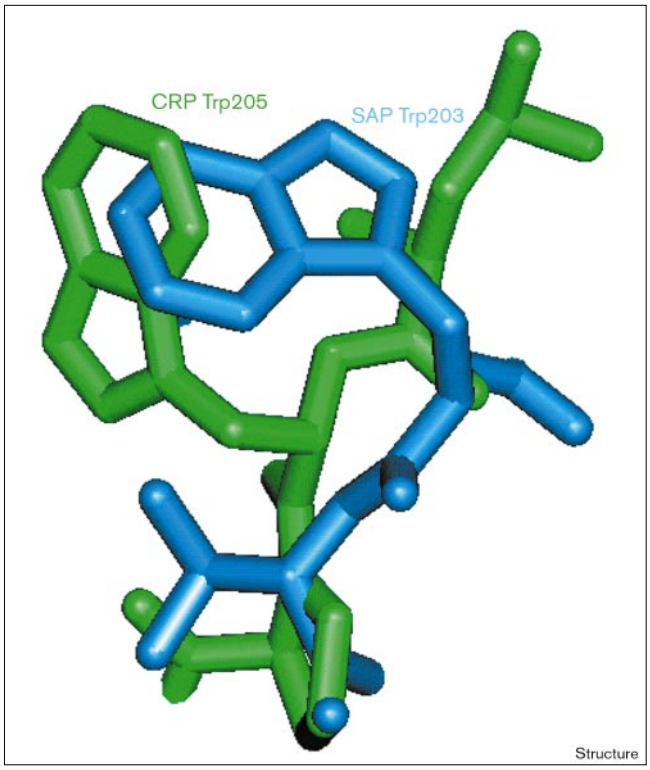

An overlay of SAP residue Trp203 (blue) and CRP residue Trp205 (green), indicating the reorganisation of the two residues.

of residue 139, but Asp60 provides only one oxygen ligand to the calcium ion (total of five ligands). The equivalent site 2 residues include Gln138, Asp140 and Gln150. Residue Glu147 (Asp145 in SAP) extends sufficiently to close the pocket with an additional bond to calcium (four ligands total), although in the 1gnh structure of CRP the sidechain of Glu147 is not positioned to coordinate the calcium ion. Thus, in CRP, the two calcium-binding sites, which are of equal affinity in solution [32], are differentiated by one carbonyl oxygen ligand and are equally occupied in the crystal. When both calcium sites are vacant in CRP, residues 140–150 form a large loop away from the body of the molecule [26], exposing an otherwise hidden site of proteolysis. In SAP, site 2 loses calcium most readily, but subunits containing a single calcium have an unchanged structure (unpublished results), indicating that site 1 interactions through Asp140 are required to stabilise the folded state of this loop.

The phosphocholine-binding site

Initial difference maps calculated from reflection data sets collected from the crystals grown in the presence of PC showed very good density for one molecule of PC in each of the five subunits of CRP (Figure 5a) [33]. The major interaction between CRP and PC occurs between the phosphate group of PC and the bound calciums. Two of the oxygens interact directly with each calcium, leaving the third oxygen pointing away from the binding site and into the solvent. This orientation would allow CRP to bind PC when the phosphate moiety is in ester linkage with other molecules. The remaining part of the PC molecule extends from this site and runs along the surface of CRP, packed against Phe66, towards the sidechain of residue Glu81 (Figure 5b). The distance between the positively charged quaternary nitrogen of PC and the acidic sidechain of Glu81 is 3.8 Å, suggesting that this interaction is an important determinant of PC binding. In SAP, the equivalent residue, the positively charged Lys79, would not favour this arrangement. Furthermore, Tyr74 of SAP would clash with the trimethyl ammonium group of PC. In CRP, this residue is Thr76, the small sidechain of which leaves a hydrophobic cavity ($8.7 \times 7 \times 3.5$ Å^3) on the surface of CRP lined by atoms from Glu81, Gly79, Asn61 and Thr76 (Figure 6). The existence of this pocket encourages design of branched PC analogues with bulky substituents at the 2 position that could be bound with higher affinity than PC. These would be powerful reagents to investigate CRP function as well as having the potential as drugs to block possible harmful effects of CRP *in vivo*. These results are in general agreement with earlier molecular modelling studies [28].

Figure 5

The binding of phosphocholine to C-reactive protein. **(a)** Difference Fourier map at 2.5 Å resolution, contoured at 2σ, showing the positions of the two calcium ions (orange) and a molecule of phosphocholine. **(b)** GRASP representation of CRP illustrating the positions of the five bound molecules of phosphocholine (orange and black).

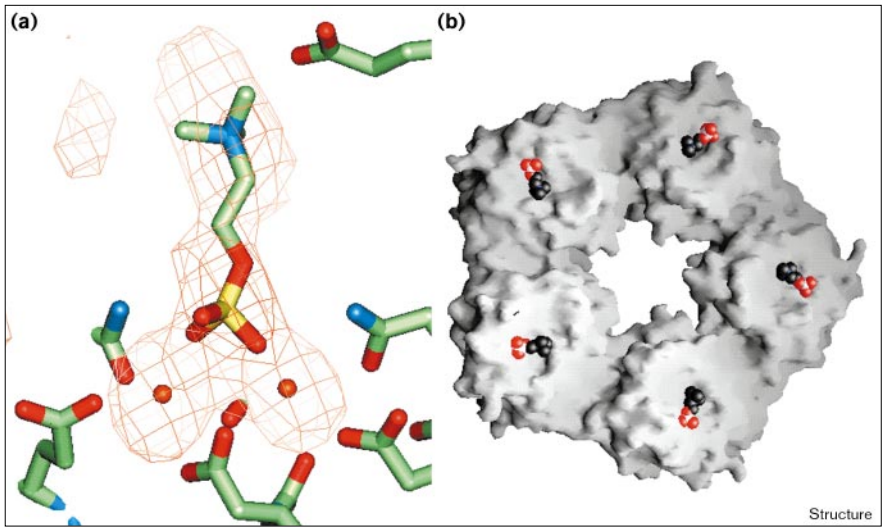

Comparison of human CRP and other pentraxins

The CRP structure complexed with PC showed the major interactions to occur between two phosphate oxygens and the calciums and the positively charged quaternary nitrogen of PC and the negatively charged sidechain of Glu81. This residue is Lys79 in SAP and would therefore not favour this arrangement. Furthermore, Tyr74 of SAP would clash with the trimethyl ammonium group of PC. This is Thr76 in CRP. This explains the failure of SAP to bind PC with high affinity. When the structure of CRP complexed with PC is superimposed onto a structure of SAP complexed with phosphoethanolamine, the phosphoethanolamine molecule is shown to interact with the calcium ions in the same way as PC, but then the remaining part of the molecule follows a different direction and heads towards Glu66 (Ser68 in CRP). The nitrogen end of PE is held in place by this residue via a water molecule that is bound between the nitrogen and Glu66. The SAP from female hamster is able to bind both amyloid and PC, thus combining the specificities of human SAP and CRP [34]; however, Tyr74, which would obstruct PC binding by SAP, is retained in hamster whereas Glu81 is replaced by Gly. Glu66 present in human SAP is retained in hamster SAP and may act as the point of interaction for the quaternary nitrogen of PC. Due to the substitution of Lys79 in human SAP with Gly in hamster SAP, there is space and flexibility in the mainchain to allow repositioning of Tyr74 to remove the steric limitation on PC binding, and Tyr74 may be positioned in an orientation that allows van der Waals contacts with PC, guiding the molecule towards Glu66.

Another difference in ligand specificity between SAP and CRP is the ability of SAP to bind the cyclic acetal of galactose, methyl 4,6-*O*-(1-carboxyethylidene)-β-D-galactopyranoside (M*O*βDG). There are only two significant differences between the proteins in the region of SAP at which M*O*βDG is bound. The interaction between the sidechain of SAP Lys79 and M*O*βDG cannot be satisfied by CRP Glu81, and van der Waals contacts to M*O*βDG provided by SAP Trp74 are not available from CRP Thr76. The presence of these different residues is therefore likely to be responsible for the failure of CRP to bind M*O*βDG.

Figure 6

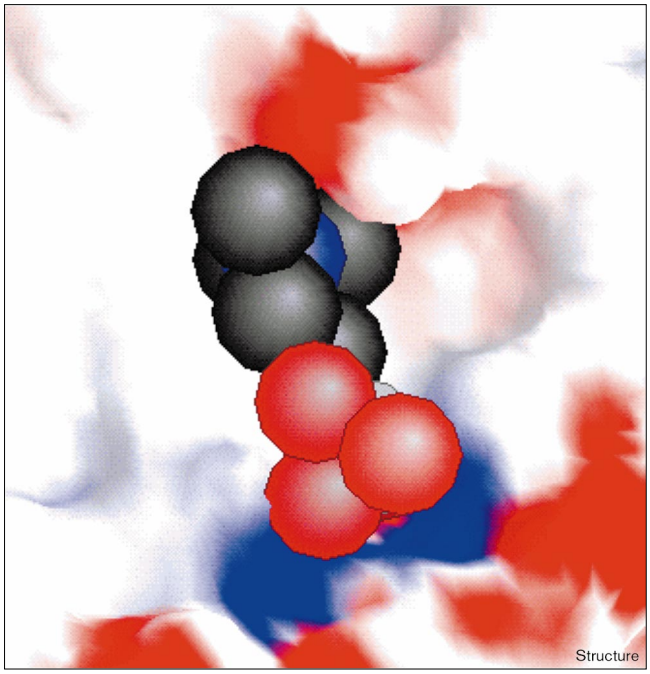

GRASP representation of the phosphocholine-binding site showing the vacant pocket adjacent to the ligand.

Figure 7

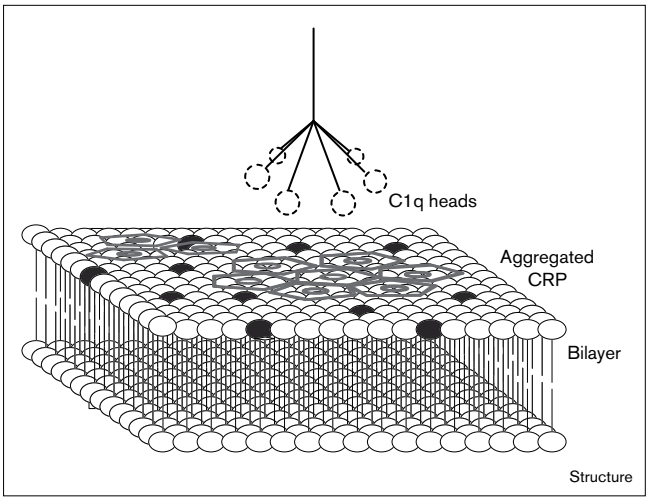

CRP (black pentagons) binds via the B face calcium sites to PC head groups of phospholipids on membranes perturbed by the action of phospholipase to produce lysolipids (black), the stability of the complex being determined by the cooperative fivefold repetition of the interaction and the high two-dimensional (2D) concentration of ligands. CRP molecules are known from electron microscopy to form ordered 2D arrays at surfaces and this effect is likely to occur on the lipid bilayer, as has been shown for Annexin V [50]. A number of proteins, including phospholipase Cβ, phospholipase A2, rabphilin 3A and synaptotagmin I, interact with cell membranes in a calcium-dependent manner via their Greek-key C2 domains [51–54]. Adjacent bound CRP molecules may present multiple binding sites via the A face furrows and central pore region for the head groups of C1q arms, providing a mechanism for head group cross-linking that is known to be involved in Fc activation of C1q by immune complexes and an explanation for the observed requirement that CRP be aggregated to the level of dimers or trimers for *in vitro* activation of complement. Highly basic peptides from the C1q A chain (76–92 and 14–26) are involved in the interaction [20]. Aggregated SAP also activates complement, but in the context of the above model we know that the B face ligand specificity is different, the spatial disposition of the binding sites is different, the architecture of the A face is modified and the pore is lined by five lysines (K87) at similar positions to the Asp112 of CRP, suggesting that these activation reactions are expressed in quite distinct biological contexts. The long pentraxin PTX3 also binds C1q via its pentraxin homology domain when in its native oligomeric state but the protein does not share the calcium and other ligand binding properties of SAP and CRP [55]. Residues H95 and W187 are the only conserved cleft residues in pentraxins binding C1q.

There are several small differences between the structure described here and that published by Shrive *et al.* (PDB code – 1gnh) [26], which includes sidechains where the electron density is expected to be less well defined, for example, Arg58, Lys31, Lys114 and Arg116. In the case of Arg116, this leads to the removal of an intersubunit ion pair with Glu42 of an adjacent protomer present in 1gnh and its replacement by a hydrogen bond to the mainchain of residue Glu85 of the same subunit in this work. In areas of stronger electron density, we find that Phe180 differs in orientation by a rotation of 180° about the Cα–Cβ bond compared to 1gnh. The protomers of this structure (1 gnh) that had calcium bound had an rms difference of 0.36 Å compared to the CRP structure described here. However, this figure increased to 1.74 Å when the 1gnh protomers without calcium were compared to the protomers described in this paper. The extent of subunit rotations are similar in all of the structures.

A model for CRP-mediated binding of C1q to the cell surface

The micromolar affinities of the pentraxin subunits for their respective small molecule univalent ligands are modest. The presence of multiple equivalent binding sites on a pentamer can, however, facilitate formation of rather stable complexes, as seen in the BB face-to-face decamers of SAP produced through base stacking of bound dAMP molecules [35]. It is not currently known to what extent the pentameric array of binding sites may contribute to amyloid recognition for SAP, but multisite interactions can be readily visualised in the binding of CRP to phospholipid PC headgroups in cell membranes.

Cells undergoing apoptosis and even nonirremediably damaged cells show flip-flop exchange between the inner and outer leaflets of the lipid bilayer, which is permissive for phospholipase action in producing lysolipids. CRP binds only to damaged plasma membranes, in which there is an increased proportion of lysophospholipid, and can then activate complement, presumably to promote beneficial and scavenging functions, but also possibly to enhance tissue injury [36–39]. The elements of CRP–ligand recognition discussed here can be assembled into a working hypothesis of the mode of targeting complement attack to compromised cells and this is presented in cartoon form in Figure 7. Similar considerations may apply to the binding of CRP and its scavenging and immunosuppressive functions [40] with regard to small nuclear ribonucleoprotein particles, the unique nuclear constituent to which CRP specifically binds under physiological extracellular ionic strength conditions [7,8]. SAP is the main chromatin and DNA-binding protein of the plasma [41], and the recent discovery in SAP knockout mice that one of its major functions is to prevent anti-chromatin autoimmunity [42] refocuses attention on the well-known defect in CRP response to the inflammatory pathology of human systemic lupus erythematosus [43]. Small nuclear ribonucleoprotein particles are strong candidate autoantigens for the induction of autoantibodies cross-reactive with double-stranded DNA [44], and the mode of binding of CRP and its effects are therefore of considerable interest with respect to the handling of these autoantigens and the pathogenesis of antinuclear autoimmune disease.

Investigation of these CRP functions is in progress through the structural analysis of additional CRP–ligand complexes, coupled with protein engineering studies to define ligand-binding mechanisms and facilitate drug design.

Biological implications

C-reactive protein (CRP), named for its binding to pneumococcal somatic C-polysaccharide, is the classical acute phase protein, the concentration of which increases in response to tissue injury, infection and inflammation. Serum CRP assays are universally used to monitor disease activity and response to therapy. CRP belongs to the highly conserved pentraxin protein family and contributes to innate immunity against infection and to handling of autologous ligands, probably helping to prevent development of autoimmunity. The autologous ligands of CRP include phospholipids and ribonucleoproteins from necrotic and apoptotic cells. CRP binds phosphocholine with the highest affinity and we describe here for the first time the precise molecular mechanism of this interaction.

Complexed or aggregated CRP activates complement, with pro-inflammatory effects, and recent observations have focused attention on a possible pathogenetic role of CRP. Firstly, it has been discovered that increased levels of CRP strongly predict the thrombo-occlusive complications of atherosclerosis, especially myocardial infarction. Secondly, CRP levels after myocardial infarction can predict complications and outcome, including death. CRP itself is deposited in the infarcted tissue and it activates complement. This presumably promotes beneficial and scavenging functions, but it also enhances tissue injury. Inhibition of this effect of CRP is thus an attractive therapeutic target.

On the basis of the elements of phosphocholine ligand recognition by CRP reported here, we suggest a possible mode of targeting complement activation to compromised cells. Similar considerations may apply to the binding of CRP to its bacterial ligands and to the autologous cellular components that are the putative foci of its scavenging and immunosuppressive functions. Furthermore, the present structural solution will assist development and refinement of inhibitors of CRP binding for use as drugs.

Materials and methods

Crystallisation

Human CRP was prepared as described previously [37]. Bi-pyramid crystals, approximately $1 \times 0.4 \times 0.4$ mm for both forms, were grown by the hanging-drop vapour-diffusion method. The drop, made up of a 1:1 ratio of CRP (40 mg/ml):well solution, was equilibrated against a well solution of 60 mM HEPES buffer (pH 7.6), 140 mM NaCl, 10 mM calcium acetate and 10% v/v MPD. In the absence of ligand, the crystal was of space group $P4_32_12$ with cell dimensions $a = b = 190.31$, $c = 132.12$ Å.

Crystals of similar morphology were grown under the same conditions as above but in the presence of 100 mM PC. These were of similar cell dimensions to those described above: $a = b = 193.94$, $c = 134.43$ Å, but were in space group $P4_12_12$ (Crystal form II). In both cases, the selection of the enantiomorph was based on strong and unequivocal translation function peaks.

Data collection and processing

Data were collected from the first crystal form using a 300 mm Mar image plate mounted on a rotating anode. These crystals diffracted to a resolution of 3.0 Å. Data were collected from the second crystal form at CLRC Daresbury PX 9.6, $\lambda = 0.89$ Å with a 300 mm Mar image plate. This crystal was frozen in a stream of cold nitrogen gas at 100°K (Oxford Cryostreams) and diffracted to a resolution of 2.5 Å. In each case, 90 images were collected, each covering 1° of rotation. Both data sets were processed with the program MOSFLM [45] and programs from the CCP4 suite. A summary of the data statistics is shown in Table 1.

Table 1

Refinement statistics.

Form	I	II
Z	2	1
Data resolution	3 Å	2.5 Å
Completeness (%)	94.6	97.6
Highest shell (%)	92	94.5
Multiplicity	3.6	4.3
I/σI	8.9	10.1
R_{merge} (%)	6.3	6.8
R_{ref} (%)	18.6	19.6
free (%)	23	24.2
Space group	$P4_32_12$	$P4_12_12$
Cell (Å)	A = B = 190.31 C = 132.12	A = B = 193.94 C = 134.43
Number. of reflections	46,391	86,545
Rms bond lengths (Å)	0.012	0.01
Rms bond angles (°)	1.7	1.5

Obtaining the phases with molecular replacement (Form I)

X-PLOR [46] was initially used to calculate the cross rotation function, with a pentamer of SAP being used as the search model. This was followed by Patterson correlation refinement. This failed to produce a significant peak, as did the program Amore [47]; however, when Patterson correlation refinement [46] was performed on the solutions obtained from Amore, a significant solution was observed that allowed translation parameters to be calculated. This peak was nineteenth in the list originally output from Amore. X-PLOR was used to calculate the translation function and produced a peak 16 sigma above the mean. This peak was only observed after the Patterson correlation refinement was performed on the rotation solution, which had the effect of rotating the protomers of SAP into positions similar to that of CRP. The orientation of the second pentamer was estimated from a self rotation function map and its translation parameters determined using a reoriented copy of the first pentamer.

Obtaining the phases with molecular replacement (Form II)

Crystal form II was readily solved by molecular replacement using the form I structure as the search model and the translation function to establish the enantiomorph. For both structures, the appearance in initial electron density maps of two calcium atoms that had been excluded from the search model provided support for the solution.

Model building and refinement

The model was rebuilt from the SAP coordinates using the program O [48] and averaged maps calculated using programs from the CCP4 suit. Refinement was carried out with data to the highest resolution available. X-PLOR was used in both instances. The final R factor for the CRP–calcium structure was 18.6% and the final R-factor for the CRP–calcium–PC structure was 19.6%. The program PROCHECK [49] was used to analyse the stereochemistry of the models and showed no residues in the disallowed regions of a Ramachandran plot. A summary of the refinement statistics is shown in Table 1.

Accession numbers

The atomic model coordinates for the structure described in this paper have been deposited with the Brookhaven Protein Data bank with accession code 1b09.

Acknowledgements

This work was supported in part by MRC Programme Grant G97900510 to MBP and by Project Grants to SPW and MBP from MRC and The Wellcome Trust.

References

1. Pepys, M.B. & Baltz, M.L. (1983). Acute phase proteins with special reference to C-reactive protein and related proteins (pentaxins) and serum amyloid A protein. *Adv. Immunol.* **34**, 141-212.
2. Pepys, M.B. (1995). The acute phase response and C-reactive protein. In: Weatherall DJ, Ledingham JGG, Warrell DA, eds. Oxford Textbook of Medicine. Third ed. Oxford: Oxford University Press, 1527-1533.
3. Pepys, M.B., Dash, A.C., Fletcher, T.C., Richardson, N., Munn, E.A. & Feinstein, A. (1978). Analogues in other mammals and in fish of human plasma proteins C-reactive protein and amyloid P component. *Nature* **273**, 168-170.
4. Pepys, M.B. (1994). Amyloidosis. In: *Samter's Immunologic Diseases. Fifth ed.* (Frank, M.M., Austen, K.F., Claman, H.N., Unanue, E.R., eds), pp. 637-655, Little, Brown and Company, Boston.
5. Pepys, M.B., Booth, D.R., Hutchinson, W.L., Gallimore, J.R., Collins, P.M. & Hohenester, E. (1997). Amyloid P component. A critical review. *Amyloid Int. J. Exp. Clin. Invest.* **4**, 274-295.
6. Volanakis, J.E. & Kaplan, M.H. (1971). Specificity of C-reactive protein for choline phosphate residues of pneumococcal C-polysaccharide. *Proc. Soc. Exp. Biol. Med.* **136**, 612-614.
7. Du Clos, T.W. (1989). C-reactive protein reacts with the U1 small nuclear ribonucleoprotein. *J. Immunol.* **143**, 2553-2559.
8. Pepys, M.B., Booth, S.E., Tennent, G.A., Butler, P.J.G. & Williams, D.G. (1994). Binding of pentraxins to different nuclear structures: C-reactive protein binds to small nuclear ribonucleoprotein particles, serum amyloid P component binds to chromatin and nucleoli. *Clin. Exp. Immunol.* **97**, 152-157.
9. Liuzzo, G., *et al*., & Maseri, A. (1994). The prognostic value of C-reactive protein and serum amyloid A protein in severe unstable angina. *N. Engl. J. Med.* **331**, 417-424.
10. Thompson, S.G., Kienast, J., Pyke, S.D.M., Haverkate, F. & van de Loo, J.C.W. (1995). Hemostatic factors and the risk of myocardial infarction or sudden death in patients with angina pectoris. *N. Engl. J. Med.* **332**, 635-641.
11. Kuller, L.H., Tracy, R.P., Shaten, J. & Meilahn, E.N. (1996). Relation of C-reactive protein and coronary heart-disease in the MRFIT nested case control study. *Am. J. Epidemiol.* **144**, 537-547.
12. Tracy, R.P., Kuller, L.H., Psaty, B.M., Cushman, M., Meilahn, E.N. & Smith, N. (1996). C-reactive protein and incidence of cardiovascular disease in older women: the rural health promotion project and the cardiovascular health study. *Circulation* **93**, 622.
13. Haverkate, F., Thompson, S.G., Pyke, S.D.M., Gallimore, J.R. & Pepys, M.B. (1997). Production of C-reactive protein and risk of coronary events in stable and unstable angina. *Lancet* **349**, 462-466.
14. Ridker, P.M., Cushman, M., Stampfer, M.J., Tracy, R.P. & Hennekens, C.H. (1997). Inflammation, aspirin, and the risk of cardiovascular disease in apparently healthy men. *N. Engl. J. Med.* **336**, 973-979.
15. Koenig, W., *et al*., & Pepys, M.B. (1997). C-reactive protein (CRP) predicts risk of coronary heart disease (CHD) in healthy middle-aged men: results from the MONICA-Augsburg Cohort Study, 1984/85–1992. *Circulation* **96** (suppl. 1), 1-99.
16. Volanakis, J.E. & Kaplan, M.H. (1974). Interaction of C-reactive protein complexes with the complement system. II. Consumption of guinea-pig complement by CRP complexes: requirement for human Clq. *J. Immunol.* **113**, 9-17.
17. Kaplan, M.H. & Volanakis, J.E. (1974). Interaction of C-reactive protein complexes with the complement system. I. Consumption of human complement associated with the reaction of C-reactive protein with pneumococcal C-polysaccharide and with the choline phosphatides, lecithin and sphingomyelin. *J. Immunol.* **112**, 2135-2147.
18. Siegel, J., Rent, R. & Gewurz, H. (1974). Interactions of C-reactive protein with the complement system. I. Protamine-induced consumption of complement in acute phase sera. *J. Exp. Med.* **140**, 631-647.
19. Volanakis, J.E. (1982). Complement activation by C-reactive protein complexes. *Ann. N.Y. Acad. Sci.* **389**, 235-250.
20. Jiang, H., Robey, F.A. & Gewurz, H. (1992). Localization of sites through which C-reactive protein binds and activates complement to residues 14-26 and 76-92 of the human C1q A chain. *J. Exp. Med.* **175**, 1373-1379.
21. Cermak, J., Key, N.S., Bach, R.R., Balla, J., Jacob, H.S. & Vercellotti, G.M. (1993). C-reactive protein induces human peripheral blood monocytes to synthesize tissue factor. *Blood* **82**, 513-520.
22. Nakagomi, A., Freedman, S.B., Lau, W. & Geczy, C.L. (1996). Procoagulant induction on human monocytes by proinflammatory stimulants is amplified by C-reactive protein and interferon-γ. *Circulation* **8**, 4063.
23. Ramani, M., Khechai, F., Ollivier, V., Ternisien, C., Bridey, F. & de Prost, D. (1995). Interleukin-10 and pentoxifylline inhibit C-reactive protein-induced tissue factor gene expression in peripheral human blood monocytes. *Thromb. Haem.* **73**, 1082.
24. McCarty, M. (1947). The occurrence during acute infections of a protein not normally present in the blood. IV. Crystallization of the C-reactive protein. *J. Exp. Med.* **85**, 491-498.
25. DeLucas, L.J., *et al*., & Bugg, C.E. (1987). Preliminary X-ray study of crystals of human C-reactive protein. *J. Mol. Biol.* **196**, 741-742.
26. Shrive, A.K., *et al*., & Greenhough, T.J. (1996). Three-dimensional structure of human C-reactive protein. *Nat. Struct. Biol.* **3**, 346-354.
27. Emsley, J., *et al*., & Wood, S.P. (1994). Structure of pentameric human serum amyloid P component. *Nature* **367**, 338-345.
28. Srinivasan, N., White, H.E., Emsley, J., Wood, S.P., Pepys, M.B. & Blundell, T.L. (1994). Comparative analyses of pentraxins: implications for protomer assembly and ligand binding. *Structure* **2**, 1017-1027.
29. Ashton, A.W., Boehm, M.K., Gallimore, J.R., Pepys, M.B. & Perkins, S.J. (1997). Pentameric and decameric structures in solution of serum amyloid P component by X-ray and neutron scattering and molecular modelling analyses. *J. Mol. Biol.* **272**, 408-422.
30. Agrawal, A. *et al*., & Volanakis, J.E. (1997). Site directed mutagenesis of the phosphocholine binding site of human C-reactive protein – role of Thr (76) and Trp (67) *J. Immunol.* **158**, 345-350.
31. CCP4 Collaborative Computational Project, Number 4, (1994). *Acta Cryst. D* **50**, 760.
32. Kinoshita, C.M., *et al*., & Gewurz, H. (1989). Elucidation of a protease sensitive site involved in the binding of calcium to C-reactive protein. *Biochemistry* **28**, 9840-9848.
33. Roux, K.H., Kilpatrick, J.M., Volanakis, J.E. & Kearney, J.F. (1983). Localization of the phosphocholine-binding sites on C-reactive protein by immunoelectron microscopy. *J. Immunol.* **131**, 2411-2415.
34. Tennent, G.A., *et al*,. & Pepys, M.B. (1993). Studies of the structure and binding properties of hamster female protein. *Immunology* **80**, 645-651.
35. Hohenester, E., *et al*., & Wood, S.W. (1997). Crystal structure of a decameric complex of human serum amyloid P component with bound dAMP. *J. Mol. Biol.* **269**, 570-578
36. Hack, C.E., *et al*., & van den Bosch, H. (1997). A role for secretory phospholipase A_2 and C reactive protein in the removal of injured cells. *Immunology Today* **18**, 111-115.
37. Vigushin, D.M., Pepys, M.B. & Hawkins, P.N. (1993). Metabolic and scintigraphic studies of radioiodinated human C-reactive protein in health and disease. *J. Clin. Invest.* **91**, 1351-1357.
38. Kushner, I. & Kaplan, M.H. (1961). Studies of acute phase protein. I. An immunohistochemical method for the localization of Cx-reactive protein in rabbits. Association with necrosis in local inflammatory lesions. *J. Exp. Med.* **114**, 961-973.
39. Kushner, I., Rakita, L. & Kaplan, M.H. (1963). Studies of acute phase protein. II. Localization of Cx-reactive protein in heart in induced myocardial infarction in rabbits. *J. Clin. Invest.* **42**, 286-292.
40. Nakayama, S., Du Clos, T.W., Gewurz, H. & Mold, C. (1984). Inhibition of antibody responses to phosphocholine by C-reactive protein. *J. Immunol.* **132**, 1336-1340.
41. Pepys, M.B. & Butler, P.J.G. (1987). Serum amyloid P component is the major calcium-dependent specific DNA binding protein of the serum. *Biochem. Biophys. Res. Commun.* **148**, 308-313.
42. Pepys, M.B. (1998). C-reactive protein and amyloidosis: from proteins to drugs? The Lumleian Lecture. In *Horizons in Medicine no. 10.* (Williams G., ed.), Royal College of Physicians, London, in press.
43. Pepys, M.B., Lanham, J.G. & de Beer, F.C. (1982). C-reactive protein in systemic lupus erythematosus. In *Clinics in the Rheumatic Diseases. No. 1* (Hughes G.R.V., ed.), pp. 91-103, W.B. Saunders Co. Ltd, Eastbourne, UK, .

44. Reichlin, M., Martin, A., Taylor-Albert, E., Tsuzuka, K., Zhang, W. & Reichlin, M.W. (1994). Lupus autoantibodies to native DNA cross-react with the A and D snRNP polypeptides. *J. Clin. Invest.* **93**, 443-449.
45. Leslie, A.G.W. (1992). Joint CCP4 and ESF-EACMB *Newsletter on Protein Crystallography No. 26,* Daresbury Laboratory, Warrington, UK.
46. Brünger, A.T. (1992). *X-PLOR Version 3.1: A system for X-Ray Crystallography and NMR*. Yale University Press, New Haven, CT.
47. Navaza, J. (1994). Amore - An automated package for molecular replacement. *Acta Cryst. A* **50**, 157.
48. Jones, T.A., Zou, J.Y., Cowan, S.W. & Kjeldgaard, M. (1991). Improved methods for building protein models in electron density maps and the location of errors in these models. *Acta Cryst. A* **47**, 110-119.
49. Laskowski, R.A., MacArthur, M.W., Moss, D.S. & Thornton, J.M. (1993). PROCHECK: a program to check the quality of protein structures. *J. Appl. Cryst.* **24**, 946-950.
50. Pigault, C., *et al.,* & Brisson, A. (1994). Formation of two dimensional arrays of Annexin V on phosphatidylserine-containing liposomes. *J. Mol. Biol.* **236**, 199-201.
51. Shao, X, *et al.*, & Rizo, T. (1996). Bipartite Ca^{2+}-binding motif in C2 domains of synaptotagmin and protein kinase C. *Science* **273**, 248-251.
52. Nalefski, E.A., *et al.,* & Clark, J.D. (1994). Delineation of two functionally distinct domains of cytosolic phospholipase A2, a regulatory Ca^{2+} dependent lipid binding domain and a Ca^{2+} independent catalytic domain. *J. Biol. Chem.* **269**, 18239-18244.
53. Yamaguchi, T., *et al.,* & Takai, Y. (1993). Two functionally different domains of Rabphilin – 3A, RAB3A p25/smg p25A-binding and phospholipid- and Ca^{2+}-binding domains. *J. Biol. Chem.* **268**, 27164-27170.
54. Davletov, B.A. & Sudhof T.C. (1994). Ca^{2+}-dependent conformational change in synaptotagmin I. *J. Biol. Chem.* **269**, 28547-28551.
55. Bottazzi, B., *et al.,* & Mantovani, A. (1997). Multimer formation and ligand recognition by the long pentraxin PTX3. *J. Biol. Chem.* **272**, 32817-32823.

Because *Structure with Folding & Design* operates a 'Continuous Publication System' for Research Papers, this paper has been published on the internet before being printed (accessed from http://biomednet.com/cbiology/str). For further information, see the explanation on the contents page.